

Mesomorphic study of novel chalconyl-ester-based nonisomeric series: Synthesis and characterization

Vinay S. Sharma & R. B. Patel

To cite this article: Vinay S. Sharma & R. B. Patel (2017) Mesomorphic study of novel chalconyl-ester-based nonisomeric series: Synthesis and characterization, *Molecular Crystals and Liquid Crystals*, 643:1, 13-27

To link to this article: <http://dx.doi.org/10.1080/15421406.2016.1262680>

 View supplementary material 

 Published online: 23 Feb 2017.

 Submit your article to this journal 

 Article views: 1

 View related articles 

 View Crossmark data 

Mesomorphic study of novel chalconyl-ester-based nonisomeric series: Synthesis and characterization

Vinay S. Sharma and R. B. Patel

Chemistry Department, K. K. Shah Jarodwala Maninagar Science College, Gujarat University, Ahmedabad, Gujarat, India

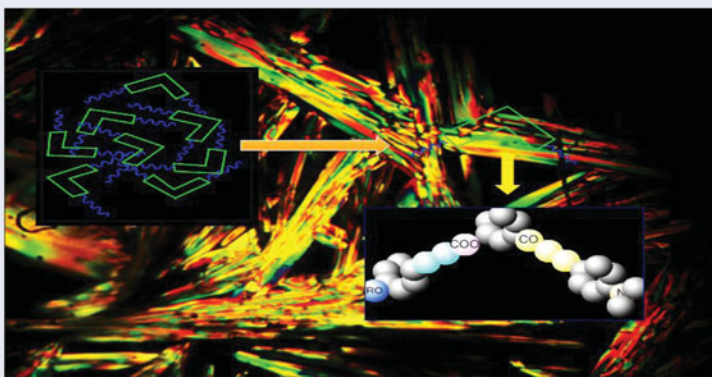
ABSTRACT

A newly designed homologues series: 3-(3-(4-(Dimethylamino) phenyl) acryloyl) phenyl 3-(4-n-alkoxyphenyl) acrylate has been synthesized and studied through chalconyl ester linking group at (meta) position. The series consists of 13 compounds, in which C_1 to C_4 homologue are nonliquid crystal, while C_5 to C_{18} exhibit nematic phase, and C_{12} to C_{18} shows smectic and nematic phase with enantiotropically manner. Mesophase image of present compounds are rod like, needle and threaded type textures investigated by POM. All this compounds were characterized by elemental analysis, FT-IR and ^1H NMR. The mesomorphism is measured by POM, DSC, and molecular packing is determined by XRD technique. The following synthesized chalconyl ester-based compounds C_5 to C_{12} shows antibacterial as well as antifungal activity compared with corresponding standard drugs. Analytical and spectral data confirmed the molecular structures of homologous series.

KEYWORDS

Antibacterial;
enantiotropically;
mesophase; nematic; smectic

GRAPHICAL ABSTRACT



1. Introduction

Liquid crystal (LC) is an intermediate state of a matter in between the solid crystalline and liquid. There are many kinds of LC materials with different molecular structures and shape. Liquid crystal is mainly divided into two category; thermotropic and lyotropic. In both of them, thermotropic liquid crystals behave a number of unique properties that have received

CONTACT Vinay S. Sharma ✉ vinaysharma3836@gmail.com 📧 Chemistry Department, K. K. Shah Jarodwala Maninagar Science College, Gujarat University, Ahmedabad 380008, Gujarat, India.

Color versions of one or more of the figures in the article can be found online at www.tandfonline.com/gmcl.

higher attention mainly due to their important role in temperature sensors, electro-optic displays, diodes, smart windows, laser and photonics, and semiconducting layers in organic field [1–4]. Thermotropic liquid crystal is formed when a solid is heated or an isotropic liquid is cooled. In addition, the molecules having an extended rod-like shape often exhibit a thermotropic liquid crystalline phase for the smectic and the nematic states proposed by Friedel et al. [5, 6]. The mesogenic behavior of lyotropic liquid crystal is exhibited in solution and depends on the concentration of solvents. In a few decades, chalconyl ester derivatives play dual role. (i) Suitable in LC devices within definite range of temperature (ii) useful in pharmaceutical preparation, anti-bacterial activity, anti-fungal, anti-malarial, anti-oxidant etc. [7–12]. Importantly, the exhibition of the liquid crystalline state of any material depends upon its molecular rigidity as well as flexibility [13–14]. Furthermore, it is also depends on molecular geometrical shape, size, aromaticity, polarity, polarizability of the terminal, lateral, and central groups, which induce suitable magnitudes of anisotropic intermolecular forces of attractions [15] as a consequence of the molecular rigidity and flexibility [16]. Liquid crystals are synthetic and biological anisotropic soft matter materials formed by an isodiametric discs, rods, V-shaped mesogenic units and amphiphiles that self-organize and assemble through the above-mentioned interactions [17, 18, 19].

In present investigation, we are going to discuss the homologous series which consisted of three phenyl rings bonded through $-\text{CH}=\text{CH}-\text{COO}-$ and $-\text{CO}-\text{CH}=\text{CH}-$ central groups as well as varying left *n*-alkoxy terminal end group and a fixed $-\text{N}(\text{CH}_3)_2$ commonly present in terminal side and its antibacterial, antifungal activity. Our group reported, LC property based on chalconyl ester linkage group [20]. The group efficiency order and structure relation with mesomorphism will be derived. According to literature, many heterocyclic-based compounds that exhibit liquid crystalline property are widely applicable in electrical, optical, biological, and medical field [21]. A number of chalcone having reported to exhibit a broad spectrum of anti-bacterial, anti-fungal, anti-ulcer, anti-malarial [23]. The presence of α , β -unsaturated functional group in chalcone ($-\text{CH}=\text{CH}-\text{CO}-$) is responsible for anti-microbial activity, which can be altered depending upon the type of substituent present on the aromatic rings [24]. Thus, in present study, we synthesized chalconyl-ester bases compounds and study mesomorphic property and its antibacterial and antifungal activity [25].

2. Experimental

2.1. Materials

For present synthesized homologous series required materials: 4-hydroxy benzaldehyde, alkyl halide (Lancaster, England, SRL Mumbai), 3-Hydroxy acetophenone, *N,N* dimethyl benzaldehyde, Malonic acid was purchased from (Sigma Aldrich), Anhydrous K_2CO_3 (Finar Chemicals, India), Dicyclohexylcarbodiimide (DCC) (Fluka) and *N,N*-dimethyl amino pyridine (DMAP) (Fluka) were used as received (Switzerland). The solvents were dried and purified by standard method prior to use.

2.2. Measurements

Melting points were taken on Opti-Melt (Automated melting point system). The FT-IR spectra were recorded as KBr pellet on Shimadzu in the range of $3800\text{--}600\text{ cm}^{-1}$. Microanalysis

was performed on Perkin-Elmer PE 2400 CHN analyser. The texture images were studied on a trinocular optical polarizing microscope (POM) equipped with a heating plate and digital camera. X-ray diffraction (XRD) were performed on a (X' PERT MPD) makes Philips, Holland. ^1H NMR spectra was recorded on a 500 MHz ^1NMR Bruker Advance- 400 in the range of 0.5 ppm-16 ppm using CDCl_3 solvent. The phase transition temperatures were measured using Shimadzu DSC-50 at heating and cooling rates of $10^\circ\text{C min}^{-1}$ it was calibrated with indium (156.6°C , 28.45 Jg^{-1}). Texture image of nematic phase were determined by a miscibility method.

2.3. Synthesis

Trans 4-n-alkoxy cinnamic acids (**B**) prepared by reported method [27]. (3-(4-(dimethyl amino) phenyl)-1-(3-hydroxy phenyl) prop-2-en-1-one (**C**) was prepared by usual established method [28]. Esters (**D**) were synthesized by a method reported in literature [29]. Thus, the Chalconyl - Ester homologue derivatives were filtered, washed with sodium bicarbonate solution, dried and purified till constant transition temperatures is obtain, using an optical POM equipped with a heating stage. The synthetic route to a series is mentioned in Scheme 1.

2.3.1. Synthesis of 4-n-alkoxy benzaldehyde (A)

4-n-Alkoxybenzaldehydes were synthesized by refluxing 4-hydroxybenzaldehyde (1 equiv.) with corresponding n-alkyl bromides (1 equiv.) in the presence of K_2CO_3 (1 equiv.) and dry acetone as a solvent [26].

2.3.2. Synthesis of trans 4-n-alkoxy cinnamic acid (B)

The resulting 4-n-alkoxybenzaldehydes were reacted with Malonic acid (1.2 equiv.) in the presence of 1-2 drops piperidine as catalyst and pyridine as solvent, refluxing the reaction mixture 3 to 4 hours to yield corresponding trans 4-n-alkoxy cinnamic acids (**B**), which was confirmed by IR study [27].

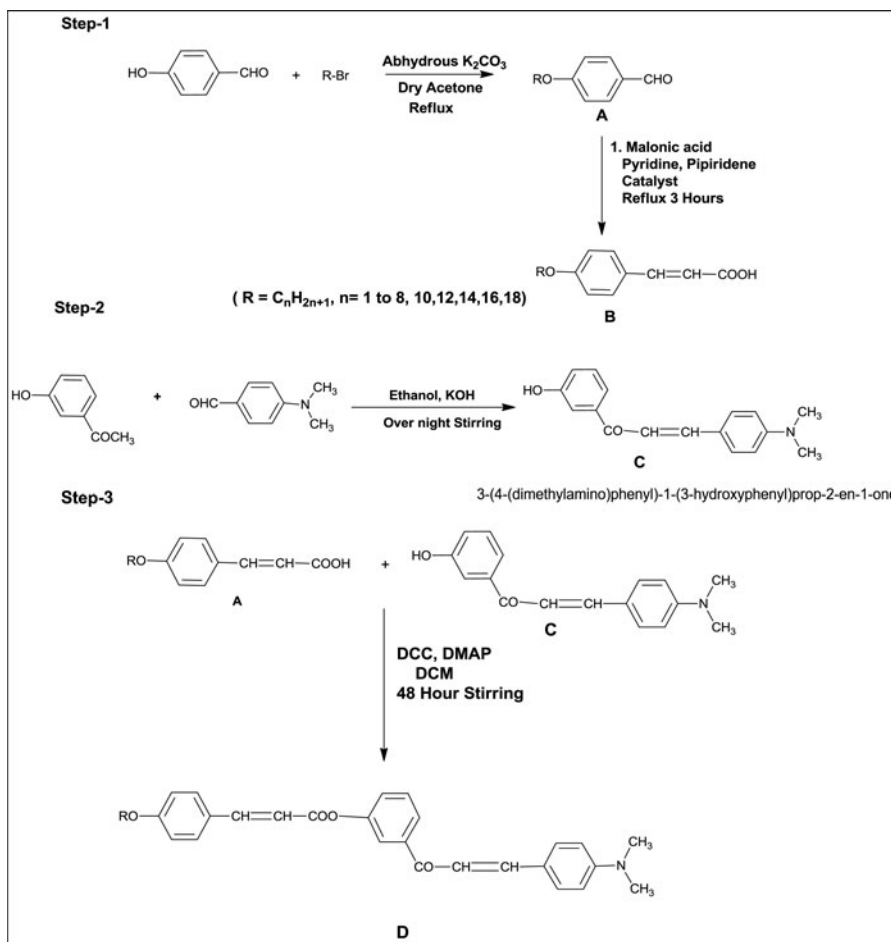
2.3.3. Synthesis of chalcone (C)

Chalcone (**C**) was prepared by usual established method reported in literature [28].

2.3.4. Synthesis of ester derivatives (D)

The compound has been prepared by esterification of the appropriate 4-n-alkoxy cinnamic acid (**A**) (2.02 mmol) and chalcone (**C**) (0.246 g, 2.02 mmol), dicyclohexylcarbodiimide (DCC) (0.457 g, 2.22 mmol) and dimethylaminopyridine (DMAP) in catalytic amount (0.002 g, 0.2 mmol) in dry CH_2Cl_2 (DCM) (30mL) was stirred at room temperature for 48 h. The white precipitate of DCU is obtained which was isolated by filtration and discarded, while the filtrate was evaporated to dryness. The resultant crude residue was purified by column chromatography on silica gel eluting with dichloromethane, recrystallization from methanol: chloroform (2:3) until constant transition temperatures were observed [28].

Reaction Scheme



Scheme 1. Synthetic procedure of series-1.

2.3.5. Analytical data

Chalcone (C): FT-IR (KBr): 3016 (-C-H- str in CH₃), 1743 (-C = O) stretch, 1512 (-C = C-) str, 1365 and 1219 (-C-O str), 979 (-C = CH), 802 di-substituted aromatic ring (meta).

Butyloxy (C₄): FT-IR (KBr): 636 Polymethylene (-CH₂-)_n of -OC₄H₉, 839(-C-H- def. di-substituted-meta), 759 Polymethylene (-CH₂-) of -OC₄H₉, 952 (-C-H- def. hydrocarbon), 1028 and 1068(-C-O-) Str, 1197 and 1228 (-C-O str in -(CH₂)_n chain, 1427 and 1427 (-C-H- def. in CH₂)1514 (-C = C-)str, 1604 and 1666 (-C = O group), 1726 (-COO- ester group), 2850 and 2970 (-C-H str in CH₃). ¹H NMR: δH (CDCl₃, 400 MHz): 0.85-0.88 (t, 3H, -CH₃ of -OC₄H₉ group), 1.36-1.38 (m, 2H, CH₃-CH₂-(CH₂)₂-O-), 1.41 (p, 2H, -CH₂-CH₂-CH₂-O-), 3.08 (s, 6H of -N(CH₃)₂), 4.00-4.02 (t, 2H, -CH₂-O-), 7.28-7.31 (d, 1H, -CH = CH-COO-), 6.50 (d, 1H, -CH = CH-COO-), 6.93-6.95 (d, 1H, -CO-CH = CH-), 7.53-7.55 (d, 1H, -CO-CH = CH-), 6.84-6.85 & 7.75-7.80 (4H, left side phenyl ring), 7.42-7.46 & 8.01-8.08 (4H, central phenyl ring), 6.68-6.10 & 7.70-7.75 (4H, terminal phenyl ring side). Elemental analysis of C₃₀H₃₁NO₄: Calc: C; 76.75%, H; 6.60%, O; 13.64%, N; 2.98%, Found: C; 76.70%, H; 6.53%, O; 13.70%, N; 2.90%.

Propyloxy (C₃): FT-IR (KBr): 628 Polymethylene (-CH₂-)_n of -OC₃H₇, 3020 (C-H Str. of alkene disubstituted), 839 (-C-H- def. di-substituted- meta), 2924-2866 (C-H Str. of poly methylene group of -OC₃H₇), 1068 (-C-O), 1726 (C = O Str. of Carbonyl carbon of (-COO- ester group), 1629 (C = C Str. of aromatic ring), 1309 (C-H bending of alkene). ¹H NMR: δH (CDCl₃, 400 MHz): 0.85-0.88 (t, 3H, -CH₃ of -OC₃H₇ group), 1.31 (q, 4H, of -CH₂ of -CH₃-CH₂-CH₂-O-), 1.34-1.39 (m, 2H, CH₃-CH₂-CH₂-O-), 1.42 (p, 2H, CH₃-CH₂-CH₂-O-), 3.08 (s, 6H of -N(CH₃)₂), 4.00-4.02 (t, 2H, -CH₂-O-), 7.28-7.31 (d, 1H, -CH = CH-COO-), 6.50 (d, 1H, -CH = CH-COO-), 6.90-6.91 (d, 1H, -CO-CH = CH-), 7.51-7.52 (d, 1H, -CO-CH = CH-), 6.82-6.86 & 7.72-7.82 (4H, left side phenyl ring), 7.40-7.48 & 8.01-8.07 (4H, central phenyl ring), 6.67-6.12 & 7.71-7.78 (4H, terminal phenyl ring side). Elemental analysis of C₂₉H₂₉NO₄: Calc: C; 76.48%, H; 6.37%, O; 14.06%, N; 3.07%, Found: C; 76.44%, H; 6.30%, O; 13.90%, N; 2.98%.

Octyloxy(C₈): FT-IR (KBr): 640 Polymethylene (-CH₂-)_n of -OC₈H₁₇, 725 Polymethylene (-CH₂-)_n of -C₈H₁₇ 817(-C-H- def. di-substituted -meta), 987 (-C-H- def. hydrocarbon), 1068 (-C-O-) Str, 1344 and 1271, 1186 (-C-O) str in -(CH₂)_n chain, 1344 and 1435 (-C-H- def. in CH₂), 1531(-C = C-)str, 1622 (-C = O group), 1732 (-COO- ester group), 2850 and 2927(-C-H str in CH₃). ¹H NMR: δH (CDCl₃, 400 MHz): 0.85-0.88 (t, 2H, -CH₃ of -OC₈H₁₇ group), 1.31 (q, 3H, -OC₈H₁₇), 1.36-1.38 (m, 2H, CH₃-CH₂-(CH₂)₆-O-), 1.42 (t, 2H, -CH₂-CH₂-CH₂-O-), 1.72 (p, of -CH₂ of -OC₅H₁₁), 3.08 (s, 6H of -N(CH₃)₂), 4.00-4.06 (t, 2H, -CH₂-O-), 7.28-7.31 (d, 1H, -CH = CH-COO-), 6.50 (d, 1H, -CH = CH-COO-), 6.93-6.95 (d, 1H, -CO-CH = CH-), 7.53-7.55 (d, 1H, -CO-CH = CH-), 6.84-6.85 & 7.75-7.80 (4H, left side phenyl ring), 7.42-7.46 & 8.01-8.08 (4H, central phenyl ring), 6.68-6.10 & 7.70-7.75 (4H, terminal phenyl ring side). Elemental analysis of C₃₄H₃₉NO₄: Calc: C; 77.71%, H; 7.42%, O; 12.19%, N; 2.66%, Found: C; 77.67%, H; 7.38%, O; 12.17%, N; 2.62%.

Heptyloxy (C₇): FT-IR (KBr): 680 Polymethylene (-CH₂-)_n of -OC₇H₁₅, 817 (-C-H- def. di-substituted meta), 3037 (C-H Str. of alkene di-substituted), 2920 (C-H Str. of poly methylene group of -OC₇H₁₅), 1720 (C = O Str. of Carbonyl in ester group), 1629 (C = C Str. of alkene), 1600, 1506 (C = C Str. of aromatic ring), 1394 (C-H bending of alkene), 968 (C-H bending of alkene). ¹H NMR: δH (CDCl₃, 400 MHz): 0.85-0.88 (t, 3H, -CH₃ of -OC₇H₁₅ group), 1.36-1.38 (m, 2H, CH₃-CH₂-(CH₂)₅-O-), 1.41 (p, 2H, -CH₂-CH₂-CH₂-O-), 4.00-4.06 (t, 2H, -CH₂-O-), 3.08 (s, 6H of -N(CH₃)₂), 7.26-7.32 (d, 1H, -CH = CH-COO-), 6.50 (d, 1H, -CH = CH-COO-), 6.93-6.95 (d, 1H, -CO-CH = CH-), 7.53-7.55 (d, 1H, -CO-CH = CH-), 6.84-6.83 & 7.72-7.80 (4H, left side phenyl ring), 7.41-7.46 & 8.01-8.08 (4H, central phenyl ring), 6.68-6.10 & 7.70-7.75 (4H, terminal phenyl ring side). Elemental analysis of C₃₂H₃₅NO₄: Calc: C; 77.26%, H; 7.04%, O; 12.87%, N; 2.81%, Found: C; 77.20%, H; 6.98%, O; 12.94%, N; 2.75%

3. Result and discussion

3.1. POM investigation

Transition temperatures (Table 2) obtained by optical cross POM equipped with a heating stage. The phase diagram plotted transition temperatures versus number of carbon atoms present in n-alkyl chain "R" of left alkyl chain (-OR) group is shown in Fig. 1. Transition curve of Cr-I follows a zigzag path of rising and falling tendency. Sm-N transition curve initially falls and passes through maxima at Tetradecyloxy (C₁₄) homologue and descends up to C₁₈ homologue. Odd-even effect is observed between C₅ to nearby C₇ homologue, odd-even effect and the alternation of transition temperature of homologues is depending

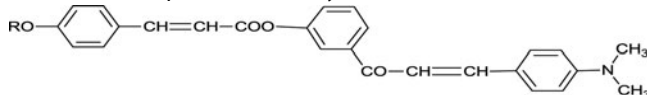
Table 1. Texture of nematic phase of C_6 , C_{14} , C_7 , C_{16} by miscibility method.

Sr. No.	Homologue	Texture
1	C_6	Schlieren
2	C_{14}	Schlieren
3	C_7	Threaded
4	C_{16}	Rod like

on odd and even number of methylene units present. Mesomorphic properties of present homologues series were varied by increasing left alkyl chain and keeping right terminal part N,N, Dimethyl $-N(CH_3)_2$ group. The geometrical shape of molecule keeping unchanged throughout the series except changing of methylene carbon units. Texture of the nematic phase observed by miscibility method (Table 1).

Presently investigated series consisted 13 (C_1 to C_{18}) homologues. C_1 to C_4 homologues are nonliquid crystal (NLC) due to short alkyl spacer. In case of higher homologue, mesophase formation is present due to long chain which increases the polarity and polarizability of molecules.

The crystalline compounds placed on clear glass slide were heated to the isotropic state and heating and cooling rate ($2^\circ C/min$), respectively, and observing mesophase texture image shown in Fig.-2, (a) for C_{10} homologue, the Sm C texture image observed at $130^\circ C$ on heating and cooling condition, (b) nematic mesophase texture of C_{12} homologue display at $148^\circ C$ enantiotropically manner, (c) rod-like mesophase image of Sm C phase for C_{16} homologue at $110^\circ C$ during heating and cooling condition, (d) rod-like textures image of Sm C phase of C_{18} homologue at $102^\circ C$ during heating and cooling conditions, respectively. In addition, we conclude that, the mesophase exhibited during heating and cooling condition. In Figure S_1 (ESI), (a) threaded type texture image of nematic mesophase for compound C_7 homologue obtained enantiotropically manner at $146^\circ C$, (b) Schlieren-type nematic phase observed at $148^\circ C$ for C_6 homologue heating as well as cooling conditions.

Table 2. Transition temperatures in $^\circ C$ by POM.

3-(3-(4-(Dimethylamino) phenyl) acryloyl) phenyl 3-(4-n-alkoxyphenyl) acrylate

Compound No	n-alkyl chain C_nH_{2n+1}	Transition Temperatures in ($^\circ C$)		
		Sm	N	I
1	C_1	—	—	240.0
2	C_2	—	—	236.0
3	C_3	—	—	190.0
4	C_4	—	—	186.0
5	C_5	—	160.0	180.0
6	C_6	—	148.0	172.0
7	C_7	—	146.0	166.0
8	C_8	—	142.0	162.0
9	C_{10}	—	130.0	158.0
10	C_{12}	126.0	146.0	156.0
11	C_{14}	120.0	137.0	150.0
12	C_{16}	110.0	130.0	144.0
13	C_{18}	102.0	120.0	132.0

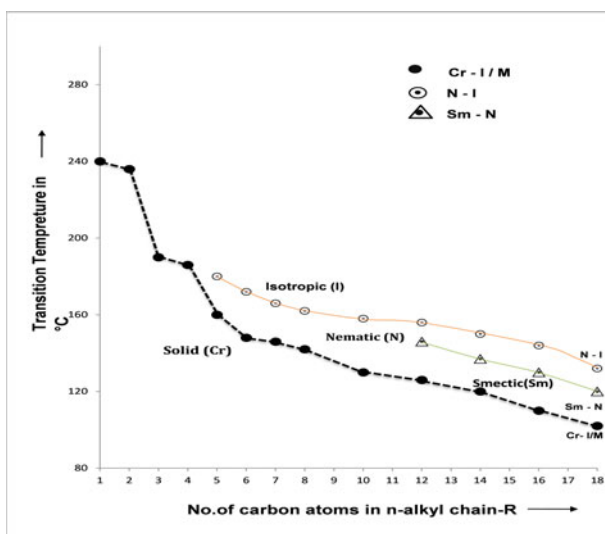


Figure 1. Phase diagram of sereis-1.

We have measured the phase sequence of C_{12} homologue at heating condition shown in Fig. 3. At room temperature (a) shows solid crystal while applying heating at 126° shows the formation of smectic phase (b), while at 146°C , nematic mesophase is observed in (c),

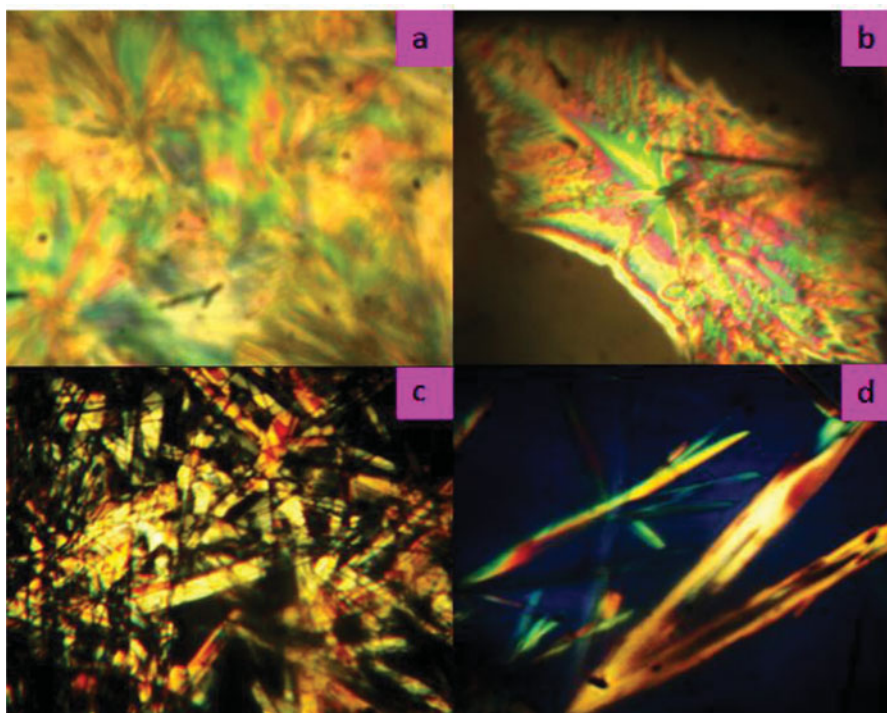


Figure 2. Mesomorphic textures of compounds obtained by POM (a) Sm C phase of C_{10} homologue on heating. (b) Nematic phase of C_{12} homologue on heating, (c) Sm C phase of C_{16} homologue on cooling, (d) Sm C phase of C_{18} homologue on heating.

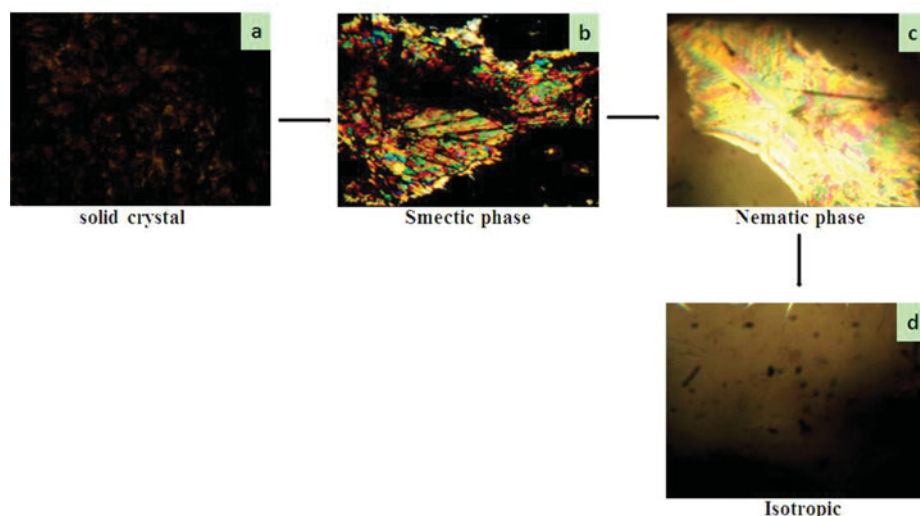


Figure 3. Phase sequence of C_{12} homologue at heating condition by POM.

isotropic of mass at 156°C during heating condition (d). Observed phase sequence is repeated again during cooled condition and also confirmed by DSC analysis.

The non-mesomorphicity of C_1 to C_4 homologue is attributed short alkyl spacer and low magnitudes of dispersion forces and lower magnitudes of dipole-dipole interaction and electronic vibrations cause high-crystalline tendency to directly transform into isotropic mass by breaking of crystal lattices. The presence of smectic phase due to increasing the chain length and increase flexibility, polarity and polarizability in which sliding moving the arrangement of molecules nearness to each other to cause smectic mesophase (C_{12} to C_{18}) homologue. Though, at cooling stage the identical mesophase is perceived. The exhibition of nematic property (C_5 to C_{18}) by appropriate magnitudes of anisotropic forces end to end attractive cohesion and closeness of molecules in statistically parallel in floating conditions that directly associated to its rigidity as well as flexibility exposed thermal vibrations.

Here, we have compared the mesomorphic property of presently investigated series-1 with structurally similar series-X, which was reported by our research group [30] mentioned in Fig.-4.

Homologous series (1) and X are identical with respect to three phenyl rings bonded through chalconyl central bridge and series 1 has more ethylene part compare to series-X. Moreover, both series-1 and X are identical with respect to left flexible n-alkoxy (-OR) group for the same homologues for desired series; but differ from homologue to homologue in the same series due to -meta substituted chalconyl linkage in series 1. However, similar terminal group in both series. Thus, they differ with respect to their geometrical shapes linearity and nonlinearity for the same homologue series to series, respectively. Hence, the variants in

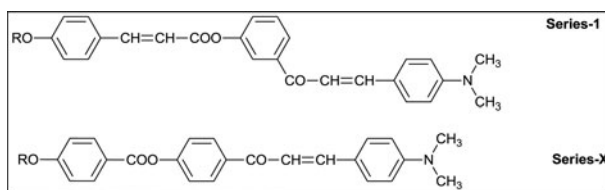


Figure 4. Structurally similar analogous series.

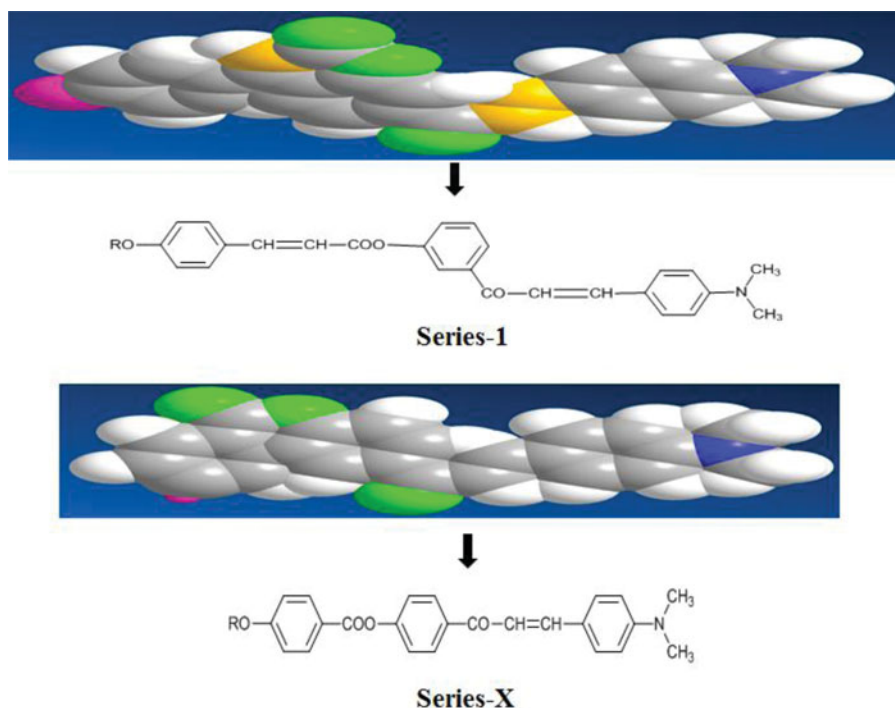
Table 3. Relative thermal stabilities in °C.

Series	1	X
Smectic-nematic Or Smectic-isotropic Commencement of smectic phase	133.2(C ₁₂ -C ₁₈)C ₁₂	59.6(C ₇ -C ₁₈)C ₇
Nematic- isotropic Commencement of nematic phase	157.7(C ₄ -C ₁₈)C ₅	76.6(C ₄ -C ₁₈)C ₄
Total upper and lower mesophase length range in °C.	20.0 to 35.0 C ₇ C ₁₆	06.0 to 35.0 C ₅ C ₁₆

mesomorphic properties for the homologue from series to series are observed due to differing magnitudes of molecular rigidity and geometry present in between series-1 and X; under comparative study.

From Table 3, it indicates that presently investigated series-1 and series-X which was chosen for comparison are smectogenic in addition to nematogenic, whereas, smectic property commences late from C₇ homologue of a series-1. However, it commences earlier from C₅ homologue by series-X. Nematic property commences from C₅ homologue in series-1 and it commences from C₄ homologue, respectively, in case of series X. Smectic and nematic thermal stability of present series 1 is higher as compared to series-X. Total upper and lower mesophase length is in increasing order from series-X to series-1. The result specifies, total thermal stability of mesophase in Series 1 is higher than series X.

The space-filling diagram indicates that the energy minimizes in both series (X) and (Y), respectively (Fig. 5). The geometrical shape of series 1 its look as bent core and its length is higher due to the presence of ethylene (-CH = CH-) with carboxy (-COO) linking group as compared to series X. Therefore, it proves that they differ with respect to combined effects of molecular rigidity and flexibility, including intermolecular distance and molecular polarizability which operates LC behaviors of series. The addition of double bond in the system increases the polarizability and length of the molecule³¹

**Figure 5.** Space filling diagram of series-1 and X.

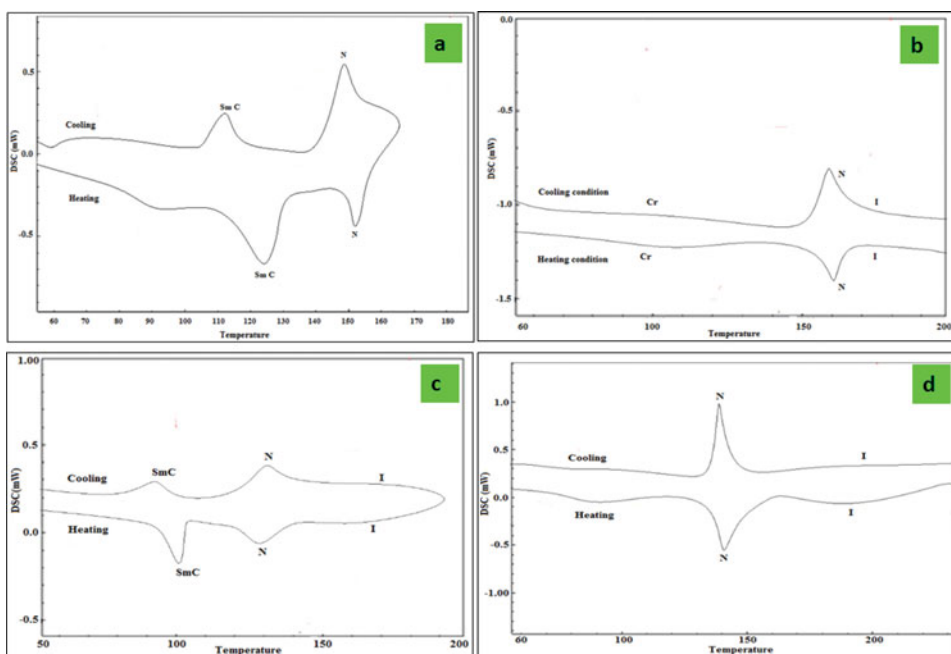


Figure 6. DSC measurement: (a) C_{12} homologue, (b) C_5 homologue, (c) C_{16} homologue, and (d) C_8 homologue.

3.2. DSC analysis

The thermal behavior of homologues series were investigated by differential scanning calorimetry (DSC). The results are shown in Fig. 6 and the value of enthalpy (ΔH) and entropy (ΔS) are mention in Table 4, (a) C_{12} homologue, heating condition first endothermic peak at 125°C , which indicates the presence of SmC. While second peak observed at 152°C shows nematic phase. At cooled condition, the endothermic peak was traced at 112°C and 148°C which was confirmed by POM. (b) C_5 homologue, one endothermic peak traced at 161.2°C in heating stage, while on cooling stage again one endothermic peak observed at 158.52 and

Table 4. Phase transition temperature ($^\circ\text{C}$) and enthalpy (J g^{-1}) and entropy change ($\text{J g}^{-1}\text{k}^{-1}$) by DSC measurement.

Comp.	Transition	Heating Peak	Cooling Peak	$\Delta H (-\text{Jg}^{-1})$	$\Delta H (\text{Jg}^{-1})$	$\Delta S (\text{J g}^{-1}\text{k}^{-1})$	$\Delta S (\text{J g}^{-1}\text{k}^{-1})$
		temperature Microscopic temperature ($^\circ\text{C}$)	temperature Microscopic temperature ($^\circ\text{C}$)				
C_{12}	Cr-SmC	125	112	22.21	20.22	0.0558	0.0508
	SmC-N	152	148	6.62	3.40	0.0155	0.0080
	N-I	164	—	—	—	—	—
C_5	Cr-SmC	130	125	31.45	34.04	0.0780	0.0885
	SmC-N	162	175	7.28	4.90	0.0167	0.0109
	N-I	170	—	—	—	—	—
C_{16}	Cr-SmC	101	95	21.42	25.12	0.0572	0.0682
	SmC-N	128	130	6.26	5.21	0.0156	0.0129
	N-I	140	—	—	—	—	—
C_8	Cr-SmC	90	—	28.66	—	0.07895	—
	SmC-N	142	138	7.49	6.39	0.0180	0.0155
	N-I	165	—	—	—	—	—

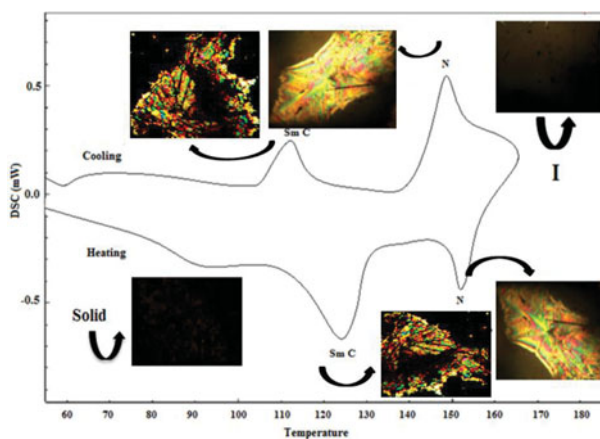


Figure 7. Phase sequence of C_{12} homologue.

second peak at 162°C during heating stage, while in cooling stage two peaks were observed at 175°C and 125°C . In POM investigation, smectic phase was not detected. However, nematic phase is confirmed. (c) C_{16} homologue, two endothermic peaks observed corresponding heating condition first endothermic peak observed at 101°C confirmed the presence of SmC and second endothermic at 128°C , that confirm the nematic mesophase. At cooling condition, two peaks are at 130°C and 95°C that indicate the presence of mesophase smectic as well as nematic phase that was also measured by POM. (d) C_8 homologue, one sharp endothermic peak observed at 142°C , endothermic peak at 90°C exhibit due to possibility of solid crystal which was confirmed by POM. At cooled condition, the single peak was traced at 138°C .

Previously in Fig. 3, we measured the phase sequence of C_{12} homologue which was confirmed by DSC analysis with trace two endothermic peaks which confirmed the presence of smectic and nematic phase at heating and cooling condition shown in Fig. 7.

3.3. XRD (X-ray diffraction) analysis

To investigate the structure of the observed smectic phase, we have performed XRD measurement to correlate with DSC and POM results (Fig. 8). According to the graphical proposed mechanism, the molecular are arranged in layers, although, the long axes of the molecules are tilted to the layers planes shown in Fig. 9. In Fig. 8, X-ray pattern show diffraction peaks in the small angle diffraction region corresponded to a smectic layer structure. A sharp low-angle peak ($2\theta = 1-4^{\circ}$), a mid-angle region peak ($2\theta = 6-9^{\circ}$) were observed during X-ray

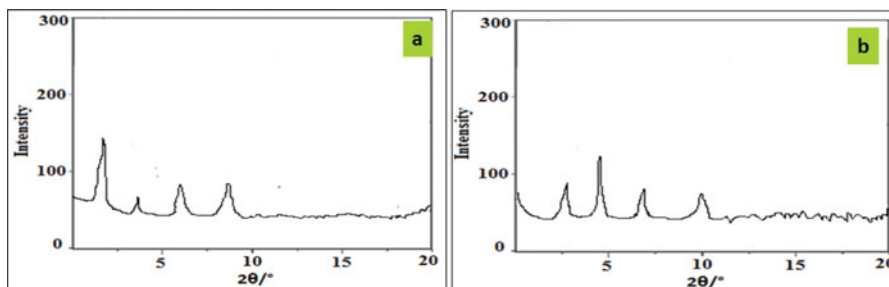


Figure 8. XRD traces of compound (a) C_6 and (b) C_8 measured at transition temperature.

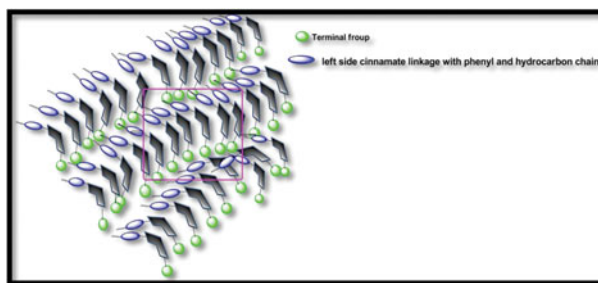


Figure 9. Representation of molecular packing of smectic phase in present series.

investigation. The reflections for the small-angle area correspond to a smectic layer structure. The d -spacing of the reflections observed for C_6 at $2\theta = 3.39, 5.4, 8.8$, were 29.42 \AA and reflections observed at $11.42 \text{ \AA}, 7.21 \text{ \AA}$, respectively, while the corresponding figures for C_8 at $2\theta = 4.80, 5.20$, and 9.82 were $31.12 \text{ \AA}, 12.13 \text{ \AA}$, and 6.42 \AA . Which is approximately nearer to its molecular length. The presence of alkyl chain in C_6 and C_8 homologue may increase the arrangement of molecules layered and induce smectic mesophase.

3.4. Biological evaluation

In the present work, the focus has been drawn on designing new structural entities of chalcones by incorporating para hydroxy acetophenone and para-substituted aldehydes into chalcone scaffolds to evaluate the prospective effect on biological activity, particular antibacterial and antifungal. Newly synthesized chalconyl-ester compounds $C_5, C_6, C_7, C_8, C_{10}, C_{12}$ were examined for antimicrobial activity against four pathogenic micro-organism viz. *E. coli*, *P. aeruginosa* (Gram –ve) and *S. aureus*, *S. pyogenus* (Gram +ve) bacterial strains. The antifungal activities were carried out with *C. albicans*, *A. niger*, and *A. clavatus* at various concentration. The synthesized compounds showed good activity results against *E. coli*, *P. aeruginosa* (Gram –ve) and *S. aureus*, *S. pyogenus* (Gram +ve). The ampicillin, gentamycin, chloramphenicol, ciprofloxacin, nystatin, and greseofulvin were used as the standard drug for gram-positive, gram-negative, and fungal strains, respectively. The minimum inhibitory concentration (MIC) was evaluated by the broth dilution method. However, in case of antifungal activity, comp. C_5, C_6, C_7, C_8 , and C_{12} showed good results in *C. Albicans* at $500 \mu\text{g/mL}$ which was equivalent to standard drug greseofulvin.

3.4.1. In vitro antibacterial activity

Table 5 shows that all the newly synthesized compounds were found to exhibit good to moderate activity against specific microbial strains. Initially, we screened all the synthesized compounds (C_5 to C_{12}) for their antibacterial activity *in vitro* by using both dilution method. The *in vitro* antibacterial results confirmed that some of the chalconyl-ester hybrids exhibited antibacterial activity against various strains of *E. coli*, *P. aeruginosa* (Gram –ve) and *S. aureus*, *S. pyogenus* (Gram +ve) as shown in Table 4. Antibacterial results were comparatively nearer to the standard drug ampicillin as compared to other drug. Compound C_5 ($125 \mu\text{g/mL}$ MIC) gives results for *E. coli* at higher concentration. While, C_6 to C_{12} showed activity ($100 \mu\text{g/mL}$ MIC) against *E. coli*, which is nearer to the standard value of ampicillin. Furthermore, compound C_{10} and C_{12} having excellent growth inhibition at lower concentration ($62.5 \mu\text{g/mL}$ MIC) as compared to standard drug. Compound C_7 to C_{12}

Table 5. Result of antibacterial activity of the synthesized compounds.

		ANTIBACTERIAL ACTIVITY			
		Minimal Inhibition Concentration			
Sr. No	Code No.	<i>E. Coli</i> MTCC 443	<i>P. Aeruginosa</i> MTCC 442	<i>S. Aureus</i> MTCC 96	<i>S. Pyogenus</i> MTCC 442
		Microgram/mL			
1	C ₅	125	120	200	200
2	C ₆	100	125	250	100
3	C ₇	100	100	250	200
4	C ₈	100	100	200	100
5	C ₁₀	62.5	100	100	62.5
6	C ₁₂	62.5	100	100	100
Standard	Ampicillin	100	100	250	100
Standard	Gentamycin	0.05	1	0.25	0.5
Standard	Chloramphenicol	50	50	50	50
Standard	Ciprofloxacin	25	25	50	50

Table 6. Result of antifungal activity of the synthesized compounds.

		ANTIFUNGAL ACTIVITY		
		Minimal Fungicidal Concentration		
Sr. No	Code. No.	<i>C. Albicans</i> MTCC 227	<i>A. Niger</i> MTCC 282	<i>A. Clavatus</i> MTCC 1323
		Microgram/mL		
1	C ₅	1000	>1000	>1000
2	C ₆	500	>1000	>1000
3	C ₇	1000	250	250
4	C ₈	500	250	250
5	C ₁₂	500	1000	1000
Standard	Nystatin	100	100	100
Standard	Greseofulvin	500	100	100

showed activity against *P. aeruginosa* at (100 µg/mL MIC), which was nearer to comparable standard drug. However, compound C₅ (120 µg/mL MIC) and C₆ (125 µg/mL MIC) showed activity at higher concentration. Compound C₁₀ exhibited good inhibitory activity with lower concentration (62.5 µg/mL MIC) against *S. Pyogenus*.

3.4.2. In vitro antifungal activity

Antifungal activity data (Table 6) displayed that the synthesized compound C₅ to C₁₂ showed adaptable degrees of inhibition against the tested fungi *C. Albicans*, *A. Niger*, and *A. Clavatus*. *C. Albicans* fungi was inhibited by C₆, C₈, and C₁₂ at 500 µg/mL MIC which is equal to the concentration of standard drug Greseofulvin. While inhibiting against *A. Niger*, *A. Clavatus* fungi by compound C₇, C₈, and C₁₂ at 200 µg/mL MIC, while all the other derivatives exerted moderate to poor activity profiles.

Conclusions

In summary, we have synthesized successfully a novel homologues series with two different linkage group containing liquid crystalline as well as antimicrobial activity. We have found that the following synthesized homologous series shows nematogenic and partly smectogenic

behavior predominantly. We have confirmed the mesogenic property for compounds by DSC and POM. Smectic phase of representative compounds were confirmed by X-ray diffractometer (XRD) at their particular transition temperature. The antibacterial and antifungal activity was determined by MIC (Broth dilution method).

Acknowledgments

Authors acknowledge thanks to Dr. R. R. Shah, principal of K. K. Shah Jarodwala Maninagar Science College, Ahmedabad. Authors are also thankful to Dr. A. V. Doshi, Ex-principal of M.V.M. Science College - Rajkot for his constant support, inspirations and help, as and when needed during the course of present investigation. Authors thank to Centre of Excellence, Rajkot for the spectral services.

References

- [1] Gelbart, W. M. (1982). *J. Phys. Chem.*, 86, 4298.
- [2] Marin, L., Damaceanu, M. D., & Timpu, D. S. (2009). *Soft Mater.*, 7, 1.
- [3] Narmura, S. (2001). *Displ.*, 22, 1.
- [4] Kim, W. S., Elston, S. J., & Ranyes, F. P. (2008). *Display*, 29, 458.
- [5] Kuang, G. C., Jia, X. R., Teng, M. J., Chen, E. Q., Li, W. S., & Ji, Y. (2012). *Chem Mater.*, 24(1), 71.
- [6] Murphy, A. R., & Frechet, J. M. J. (2007). *Chem. Rev.*, 107, 1066.
- [7] Bilalov, A., Olssona, U., & Lindam, V. (2011). *Soft Matter*, 7, 730.
- [8] Imrie, C. T. (1999). *Struct. Bond.*, 95, 149.
- [9] Cristiano, R., Vieira, A. A., Ely, F., & Gallardo, H. (2006). *Liq. Cryst.*, 33, 381.
- [10] Mills, J., Miller, R., Gleeson, H., Seed, A., Hird, M., & Styring, P. (1997). *Mol. Cryst. Liq. Cryst.*, 303(1), 145.
- [11] Marcos, M., Omenat, A., Serrano, J. L., & Ezcurra, A. (1992). *Adv. Matter.*, 4, 285.
- [12] Hird, M., Toyne, K. J., Gray, G. W., Day, S. E., & Donell, D. G. M. (1993). *Liq. Cryst.*, 15, 123.
- [13] Achalkumar, A., Rao, D. S. S., & Yelamaggad, C. V. (2014). *New J. Chem.*, 38, 4235.
- [14] Hertz, E., Lavorel, B., & Faucher, O. (2011). *Nature Photon.*, 5, 783.
- [15] (a) Shankar, G., & Yelamaggad, C. V. (2012). *New J. Chem.*, 36, 918. (b) Suthar, D. M., & Doshi, A. V. (2013). *Mol. Cryst. Liq. Cryst.*, 575, 76. (c) Chauhan, H. N., & Doshi, A. V. (2013). *Mol. Cryst. Liq. Cryst.*, 570, 92.
- [16] Khosla, S., Suman, L., Sood, N., Bawa, S. S., & Nahar, S. (2011). *Int. J. Theor. Appl. Sci.*, 3, 67.
- [17] David, P. K., & Fritz, V. (2002). *Phil. Tran. R. Soc. Lond., B.*, 357, 155.
- [18] Gray, G. W., Hird, M., Lacey, D., & Toyne, K. J. (1989). *J. Chem. Soc.*, 2, 2041.
- [19] Doric, Z., & Fraden, S. (2006). *Curr. Opin. Colloid Interface Sci.*, 11, 47.
- [20] (a) Patel, R. B., Patel, V. R., & Doshi, A. V. (2012). *Mol. Cryst. Liq. Cryst.*, 552, 3. (b) Sharma, V. S., Solanki, R. B., Patel, P. K., & Patel, R. B. (2016). *Mol. Cryst. Liq. Cryst.*, 625, 137. (c) Jain, B. B., Jadeja, U. H., Sharma, V. S., & Patel, R. B. (2016). *Mol. Cryst. Liq. Cryst.*, 625, 146. (d) Sharma, V. S., & Patel, R. B. (2015). *ILCPA., Sci. Press.*, 59, 115. (e) Sharma, V. S., & Patel, R. B. (2015). *ILCPA, Scipress.*, 58, 144. (f) Sharma, V. S., & Patel, R. B. (2015). *ILCPA., Scipress.*, 60, 182. (g) Sharma, V. S., & Patel, R. B. (2016). *ILCPA., Scipress.*, 64, 69.
- [21] Sashidhara, K. V., Rao, K. B., Kushwaha, P., Modukuri, R. K., Singh, P., Soni, I., et al. (2015). *ACS Med. Chem. Lett.*, 6, 806.
- [22] Fischer, P., & Finkelmann, H. (1998). *Prog. Colloid. Polym. Sci.*, 111, 127.
- [23] Griffin, R. J., Srinivasan, S., Bowman, K., Calvert, A. H., Curtin, N. J., Newell, D. R., Pemberton, L. C., & Golding, B. T. (1998). *J. Med. Chem.*, 41, 5247.
- [24] Dominguez, J. N., Leon, C., Rodrignes, J., Dominguez, N. G., Gut, J., & Rosenthal, P. J. (2005). *J. Med. Chem.*, 48, 3654.
- [25] Kitawat, B. S., Singh, M., & Kale, R. K. (2013). *New J. Chem.*, 37, 2541.
- [26] Hasan, A., Abbas, A., & Akhtar, M. N. (2011). *Molecule.*, 16, 7789.

- [27] Qian, Y., Zhang, H. J., Zhang, H., Xu, C., Zhao, J., & Zhu, H. L. (2010). *Bio-Organic and Med. Chem.*, 18, 4991.
- [28] Furniss, B. S., Hannford, A. J., Smith, P. W. G., & Tatchell, A. R. (1989). *Vogel's Textbook of Practical Organic Chemistry* (4th Edn.), Longmann Singapore Publishers Pvt. Ltd.: Singapore, 563–649.
- [29] Pinol, R., Ros, M. B., Serrano, J. L., & Sierra, T. (2004). *Liq. Cryst.*, 31, 1293.
- [30] Sharma, V. S., & Patel, R. B. (2016). *Mol. Cryst. Liq. Cryst.*, 630, 162.